

Blast Furnace Ironmaking Process with Super-High TiO₂ in the Slag: Sulfide Capacity



JIAWEI LING, ZHENGDE PANG, YUYANG JIANG, ZHIMING YAN, and XUEWEI LV

To increase the utilization of V-Ti-Magnetite ore in the burden of a blast furnace, we investigated replacing CaO with MgO. The high fraction of TiO₂-bearing raw materials leads to a super-high TiO₂ content in the blast furnace slag, typically above 30 wt pct, which affects normal blast furnace operation. The present study focuses on the sulfide capacity of slag containing a super-high TiO₂ content. The effects of TiO₂ content and the ratio of MgO to CaO (M/C) on the sulfide capacity of slag were examined using a gas-slag equilibrium method. In the CaO-SiO₂-TiO₂-MgO-Al₂O₃ slag system, as the content of TiO₂ in the slag increased from 20 to 34 wt pct, the sulfide capacity decreased from 6.25×10^{-5} to 2.86×10^{-5} . Above 30 wt pct TiO₂, the influence of TiO₂ content on the sulfide capacity became negligible. Increasing the (M/C) ratio induced a non-monotonic trend in the sulfide capacity, which first increased and then decreased. Thermodynamic and structural analyses were employed to characterize the experimental results. Thermodynamically, decreasing the CaO activity reduced the free oxygen in the slag with increasing TiO₂ content. Furthermore, an increase of titanium suboxide slowed the reduction of the sulfide capacity. Mass substitution mainly influenced the availability of free oxygen in the slag, and then the sulfide stability and oxygen concentration worked together, resulting in a non-monotonic sulfide capacity when MgO was substituted for CaO. In addition, the sulfide capacity was dependent on the effect of both the quaternary molar basicity and the binary molar basicity. Finally, the structural analysis revealed that for a super-high TiO₂ content in the slag, both the structure of Ti and the depolymerization reaction of Ti had an extremely important effect on desulfurization.

<https://doi.org/10.1007/s11663-021-02192-9>

© The Minerals, Metals & Materials Society and ASM International 2021

I. INTRODUCTION

THE comprehensive utilization of vanadium-titanium magnetite ore (VTM) has always been a hot topic in metallurgy research. In the blast furnace ironmaking process, significantly increasing the content of VTM can effectively improve the recovery and utilization of vanadium-titanium resources.^[1–3] Unfortunately, serious slagging difficulties, such as slag foaming and poor fluidity of the slag may occur with an increase in the TiO₂ content in blast furnace slag (BFS).^[4,5] In our previous studies,^[3,6] an innovative slag system, in which

MgO was used as a substitute for CaO, has been proposed, and some high-temperature physicochemical properties of the slag have been evaluated. Desulfurization ability is an important chemical property of BFS, and plays an essential role in determining the quality of hot metal. Sulfide capacity is the main parameter used for characterizing the desulfurization ability of slag. The sulfide capacity determines the selection of the slag desulfurization system and is also a particularly important indicator of the high-temperature physicochemical properties of slag; hence, it has received much attention in the ironmaking process.^[7–12] Therefore, this study was focused on the sulfide capacity of slag containing a super-high TiO₂ content in the blast furnace ironmaking process.

Many studies have focused on the sulfide capacity of BFS containing TiO₂, as shown in Figure 1. Ghita *et al.*^[13] measured the sulfide capacities of FeO-TiO₂-SiO₂ and FeO-TiO₂-CaO. Brown *et al.*^[14] investigated the sulfide capacity of CaO-(MgO)-TiO₂-SiO₂-Al₂O₃ slags. Both research groups found that the sulfide capacity of the slag increases with increasing content of basic oxides like FeO, MgO, and CaO. With a fixed basic oxide content, replacing SiO₂ or Al₂O₃ with TiO₂

JIAWEI LING, ZHENGDE PANG, YUYANG JIANG, and XUEWEI LV is with the Chongqing Key Laboratory of Vanadium-Titanium Metallurgy and Advanced Materials, Chongqing University, No. 174 Shazheng Street, Shapingba District, Chongqing 400044, P.R. China and also with the College of Materials Science and Engineering, Chongqing University, No. 174 Shazheng Street, Shapingba District, Chongqing, 400044 P.R. China. Contact e-mail: lvxuewei@163.com
ZHIMING YAN is with the WMG, the University of Warwick, Coventry, CV4 7AL, UK. Contact e-mail: Zhiming.Yan@warwick.ac.uk

Manuscript submitted October 21, 2020; accepted April 15, 2021.

Article published online June 11, 2021.

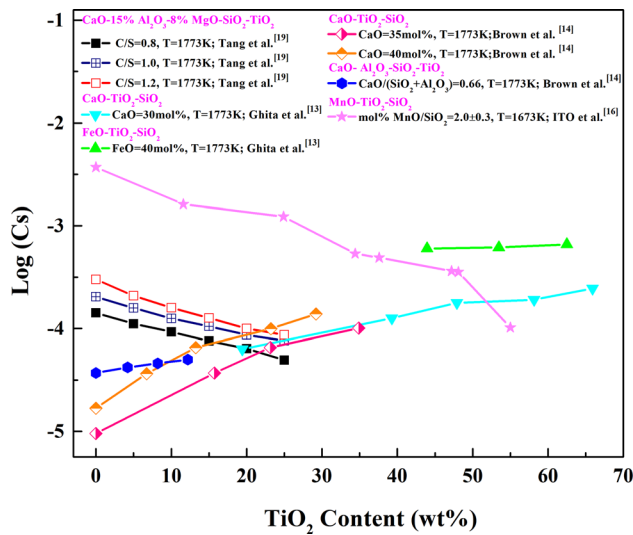


Fig. 1—Sulfide capacity of TiO_2 -bearing slags from previously published works.

may lead to increased sulfide capacity of the slag. Sommerville *et al.*^[15] summarized and compared the desulfurization capabilities of different slag systems, and concluded that the desulfurization capability of TiO_2 is lower than that of CaO , MgO , and FeO , but is higher than that of Al_2O_3 and SiO_2 . Ito^[16] reported that for the $\text{MnO-TiO}_2\text{-SiO}_2$ slag system with a fixed molar ratio of MnO/SiO_2 , increasing the TiO_2 content reduced the sulfide capacity. Che *et al.*^[17–19] found that the sulfide capacity of BFS containing TiO_2 is far inferior to that of ordinary BFS owing to the high TiO_2 content and low CaO content of the former. Tang *et al.*^[19] measured the sulfide capacity of $\text{CaO-SiO}_2\text{-TiO}_2\text{-MgO-Al}_2\text{O}_3$ by the slag-metal equilibrium method, and reported that the sulfide capacity increased with an increase in the basicity and a decrease in the content of TiO_2 in the BFS. Increasing the MgO content will improve the sulfide capacity of BFS containing TiO_2 . However, it was reported^[3,6] that MgO can affect the viscosity of BFS, and its content should not exceed 14 wt pct.

Generally, there are two main methods of measuring sulfide capacity: the slag-gas equilibrium method and the slag-metal equilibrium method.^[20] This present work studies the sulfide capacity of BFS during the region of very high TiO_2 content from 20 to 34 wt pct, which is yet to be done. Employing slag-gas equilibrium method can eliminate the effect of TiO_2 reduction by carbon in the hot metal. Therefore, using the slag-gas equilibrium method in this study, the sulfide capacity of $\text{CaO-SiO}_2\text{-TiO}_2\text{-MgO-Al}_2\text{O}_3$ slag was investigated as a function of TiO_2 content ranging from 20 to 34 wt pct and $\text{MgO wt pct/CaO wt pct}$ (M/C) ratios ranging from 0.32 to 0.65.

II. EXPERIMENTAL

A. Materials

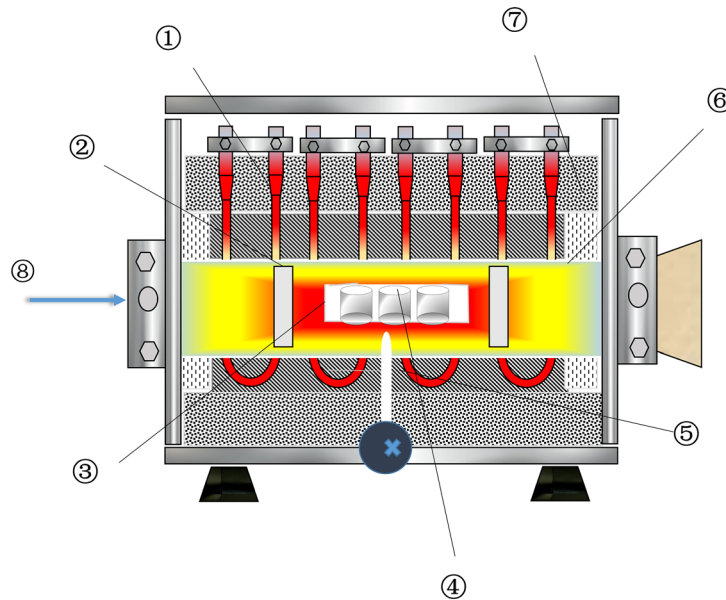
The synthetic slag was quenched with water after all the pure compounds were pre-melted. In the gas-slag equilibrium method, a mixture gas at a flow rate of 400 mL/min was introduced into the reaction chamber after passing the gas through the purification system. The gas mixture was composed of $\text{Ar-CO-CO}_2\text{-SO}_2$ (Ar : 99.99 pct purity, CO : 99.5 pct purity, CO_2 : 99.5 pct purity, SO_2 : 99.9 pct purity) with a volume ratio of 200:100:80:20. The flow rate of each gas was controlled by special mass flowmeters.

B. Experimental Procedure

The experimental setup is shown in Figure 2. The heating system consisted of electric resistance heaters, an alumina reaction tube, and a thermocouple. There were eight silicon-molybdenum heaters installed along two sides of the furnace, with a maximum operating temperature of up to 1700 °C. The constant temperature zone inside the furnace was approximately 7 cm in length. A proportional integral differential (PID) controller was used to maintain the temperature within ± 2 K. The purification system consisted of four dehydration tubes, two YJ-O100 deoxidation tubes, four special mass flowmeters, and a gas mixing chamber before entering the furnace. The dehydration tube was half-filled with color-changing silica gel and the other half was filled with molecular sieves. A YJ-O100 deoxidation tube was filled with the deoxidation agent for the palladium-catalyst oxidation system.

The time required to achieve equilibrium was established by comparing the sulfur content in the slag samples after the reaction with the mixed gas for 4, 6, and 8 hours; the results are presented in Figure 3. This indicates that the sulfur content did not vary after 6.0 hours. Hence, the optimum equilibrium time for the desulfurization reaction used for the subsequent experiment was 8 hours.

One gram of sample was weighed and placed in a platinum crucible (size: $r = 0.62$ cm, $h = 1$ cm, $\text{Pt} \geq 99.95$ pct). In one experiment, three platinum crucibles were placed on the corundum boat and were positioned in the constant temperature zone of the horizontal furnace. The samples were heated in the furnace and protected by high-purity argon after purification during the heating process. The samples were held for 8 hours at 1773 K under the experimental atmosphere for equilibrium. The furnace was then shut down and the gas was simultaneously changed to purified argon. The samples were cooled in the furnace at a cooling rate of 40 K/min to solidification. The samples were crushed to particles smaller than 100 μm , and the final sulfur content in the slag was measured by chemical titration analysis.

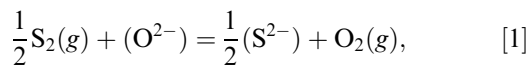


① Silicon-molybdenum bars ② Asbestos shield ③ Corundum boat ④ Platinum crucible
⑤ Platinum rhodium thermocouple ⑥ Alundum tube ⑦ Refractory ⑧ Gas purification system

Fig. 2—Sulfide capacity experimental furnace.

III. RESULTS AND DISCUSSION

The sulfide capacity (C_s) of slag equilibrated with the mixed gas is defined by Eq. [2], which is derived from Eq. [1]:



$$C_s = (\text{wt pct S}) \times \left(\frac{P_{O_2}}{P_{S_2}} \right)^{\frac{1}{2}}, \quad [2]$$

where (wt pct S) is the mass percentage of sulfur dissolved in the slag, while P_{O_2} and P_{S_2} are the partial pressures of oxygen and sulfur, respectively. The experimental partial pressure of the gases at 1773 K was calculated using the thermochemical program FactSage. The results are shown in Table I.

The chemical compositions of the samples used in the present investigation, the analyzed sulfur content in the slag, and the parameters from the sulfide capacity calculation are shown in Table II.

A. Effect of TiO_2 on the Sulfide Capacity

The effect of the TiO_2 content on the sulfide capacity is shown in Figure 4. The logarithm of the sulfide capacity decreased from -4.20 at a 20 wt pct TiO_2 content to -4.67 at a 34 wt pct TiO_2 content. The sulfide capacity declined rapidly at first with increasing TiO_2 content, and then declined gradually above 30 wt pct TiO_2 . Because the sulfide capacity of the $CaO-SiO_2-MgO-Al_2O_3-(TiO_2)$ slag system is dependent on the activity of CaO, which provides most of the oxygen ions

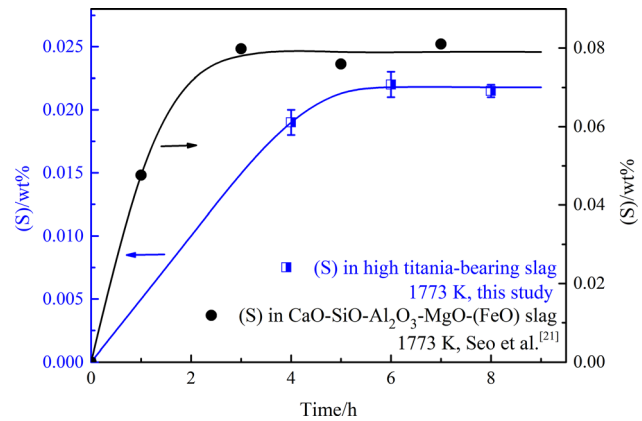


Fig. 3—Determination of equilibrium time.

Table I. Experimental Partial Pressure of Various Gaseous Species at 1773 K

Gas	Partial Pressure (atm)
Ar	5.060×10^{-1}
CO	2.039×10^{-1}
CO ₂	2.506×10^{-1}
SO ₂	2.540×10^{-2}
S ₂	1.086×10^{-2}
O ₂	3.460×10^{-8}

available for replacement by sulfur,^[21] increasing the TiO_2 content rapidly decreased the sulfide capacity of the slag. However, titanium suboxides also increase with

Table II. Weighed and Measured Chemical Composition of the Studied Slag and Sulfide Capacities at 1773K After Gas/Slag Equilibria

No.	Chemical Composition of Designed Slags (Wt Pct)					Ti ₂ O ₃	C/ S*	(C + M)/ S*	M/ C*	Sulfur content (Wt Pct) (S)	Sulfide Capacity	
	CaO	SiO ₂	MgO	Al ₂ O ₃	TiO ₂						Cs*10 ⁴	logCs
A1	30.38 (29.49)	27.62 (27.79)	8 (8.09)	14 (13.92)	20 (19.59)	(0.15)	1.1	—	—	0.035	0.625	− 4.204
A2	29.33 (28.73)	26.67 (27.19)	8 (8.14)	14 (13.77)	22 (21.55)	(0.15)	1.1	—	—	0.027	0.482	− 4.317
A3	28.29 (27.45)	25.71 (25.87)	8 (7.94)	14 (13.69)	24 (23.52)	(0.15)	1.1	—	—	0.02	0.357	− 4.447
A4	27.24 (26.49)	24.76 (25.09)	8 (7.87)	14 (13.62)	26 (25.48)	(0.18)	1.1	—	—	0.016	0.286	− 4.544
A5	26.19 (25.24)	23.81 (24.11)	8 (8.11)	14 (13.44)	28 (27.46)	(0.17)	1.1	—	—	0.014	0.250	− 4.602
A6	25.14 (24.41)	22.86 (23.13)	8 (8.08)	14 (13.19)	30 (29.36)	(0.15)	1.1	—	—	0.012	0.214	− 4.669
A7	24.10 (23.33)	21.91 (22.03)	8 (8.14)	14 (13.32)	32 (31.28)	(0.19)	1.1	—	—	0.013	0.232	− 4.634
A8	23.05 (22.57)	20.95 (21.22)	8 (8.05)	14 (13.24)	34 (33.17)	(0.21)	1.1	—	—	0.012	0.214	− 4.669
B1	25.14 (24.41)	22.86 (23.13)	8 (8.08)	14 (13.19)	30 (29.36)	(0.15)	—	1.4	0.32	0.012	0.214	− 4.669
B2	24.14 (23.39)	22.86 (23.21)	9 (9.13)	14 (13.67)	30 (29.48)	(0.17)	—	1.4	0.37	0.016	0.286	− 4.544
B3	23.14 (22.48)	22.86 (23.15)	10 (10.08)	14 (13.36)	30 (29.29)	(0.16)	—	1.4	0.43	0.018	0.321	− 4.493
B4	22.14 (21.53)	22.86 (23.2)	11 (11.2)	14 (13.27)	30 (29.3)	(0.16)	—	1.4	0.50	0.018	0.321	− 4.493
B5	21.14 (20.67)	22.86 (23.17)	12 (12.17)	14 (13.58)	30 (29.51)	(0.13)	—	1.4	0.57	0.016	0.286	− 4.544
B6	20.14 (19.7)	22.86 (23.19)	13 (12.93)	14 (13.49)	30 (29.42)	(0.18)	—	1.4	0.65	0.013	0.232	− 4.634

C/S*: CaO(wt pct)/SiO₂(wt pct) (C + M)/S*: (CaO + MgO) (wt pct)/SiO₂(wt pct) M/C*: MgO(wt pct)/CaO(wt pct).
Oxygen potential P_{O₂} = 3.460 × 10^{−8} atm, sulfur potential P_{S₂} = 1.086 × 10^{−2} atm.
Case B1 is the same as A6, and the values in parentheses are the slag compositions from XRF analysis after pre-melting.

increasing TiO₂ content and contribute to the stability of the slag. In other words, titanium suboxides can increase the sulfide capacity of the slag. Che confirmed this phenomenon, and pointed out that titanium suboxides are basic oxides, which favors the desulfurization reaction, based on a thermodynamic analysis.^[17]

Tang *et al.*^[19] reported the same tendency for the CaO-SiO₂-TiO₂-MgO-Al₂O₃ quinary slag system (Figure 4). However, the sulfide capacity was generally higher than that in this study because the basicity of that system was 1.2, which was higher than that in this study. On the other hand, more suboxides were formed in that system due to the use of the slag-metal method with a graphite crucible.

B. Effect of M/C on the Sulfide Capacity

As shown in Figure 5, the sulfide capacity of high TiO₂ slag did not follow a monotonic variation but increased and then declined as the M/C ratio increased from 0.32 to 0.65. The logarithm of the sulfide capacity increased from − 4.669 to − 4.493 between an M/C ratio of 0.32 and 0.43, and then decreased to − 4.634 at an M/

C ratio of 0.65. Unlike TiO₂, both CaO and MgO provide free oxygen. For CaO-SiO₂-Al₂O₃-MgO(-FeO) slag, the activity of CaO decreases with increasing M/C ratio, which can reduce the sulfide capacity, as reported by Seo^[22] and Karsrud.^[23,24] However, Hawkins^[25] found that mass substitution of CaO with MgO (by wt pct) enhances the sulfide capacity of slag. Because in the process of equal mass substitution, due to the difference in relative atomic mass between MgO and CaO, the molar amount of MgO increases more than the reduction of CaO. On the molar fraction scale in Table III, equal mass substitution leads to an increase in the total basic oxide content while the activity of CaO decreases, resulting in a non-monotonic sulfide capacity when MgO is substituted for CaO. Combining the dissolution behavior of sulfur in the slag allows better understanding of this non-monotonicity. Kang and Park^[26] reported that the sulfide capacity of ternary silicate slag is impacted by the sulfide stability and oxygen concentration. The stability of MgS is much lower than that of CaS, but at low basicity, MgO can provide additional free oxygen compared to CaO, and free oxygen plays a more important role than sulfide in slag stability. This

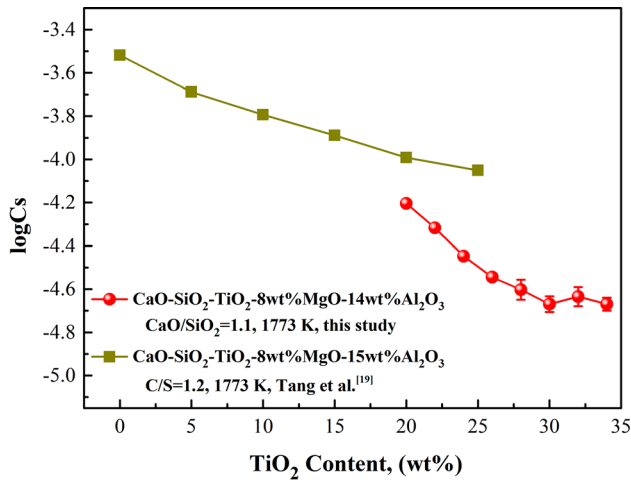


Fig. 4—Effect of TiO_2 content on the sulfide capacity of the slags at 1773 K (1500 °C).

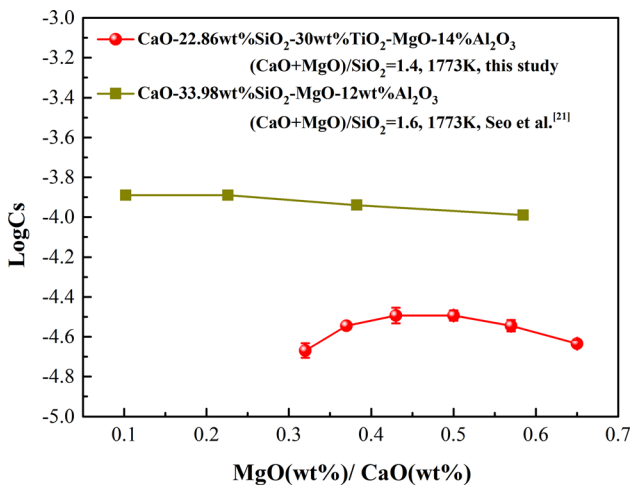


Fig. 5—Effect of M/C on the sulfide capacity of the slags at 1773 K (1500 °C).

theory can also be applied to quinary high-titanium systems, in which high-titanium plays a key role in the transition (see the detailed analysis below).

C. Thermodynamic Analysis

FactSage software is a thermodynamic calculator that has been widely used in the metallurgical slag field. The variation in the sulfur content of the slag with titanium suboxide (Ti_2O_3) under the slag-gas equilibrium condition was calculated by FactSage (Figure 6). With increasing the Ti_2O_3 content, the sulfur content in the slag increased, confirming that the Ti_2O_3 content of this slag had a positive influence on the sulfide capacity. The variation in titanium suboxide (Ti_2O_3) content with TiO_2 in this study is shown in Figure 7. Increasing the TiO_2 content increased the Ti_2O_3 content and improved the sulfide capacity to some extent, which slowed the sulfide capacity reduction rate. However, with an

Table III. Molar Fraction of the Slag With MgO Substitution of CaO

	CaO	MgO	TiO_2	(CaO + MgO)
B1	0.291	0.129	0.244	0.420
B2	0.278	0.144	0.243	0.423
B3	0.266	0.160	0.242	0.425
B4	0.253	0.175	0.241	0.428
B5	0.240	0.190	0.240	0.430
B6	0.228	0.205	0.238	0.433

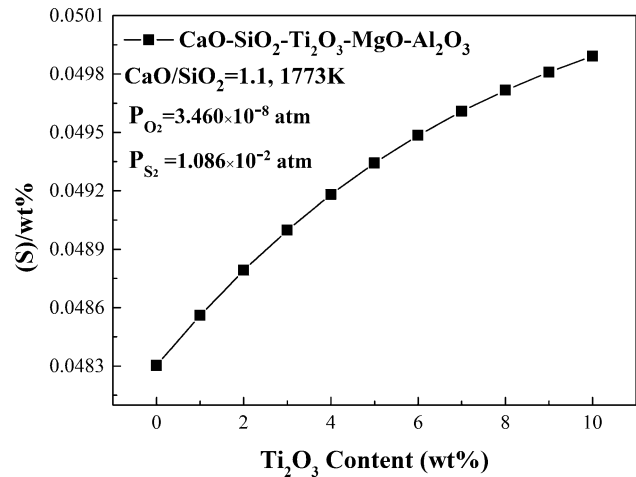
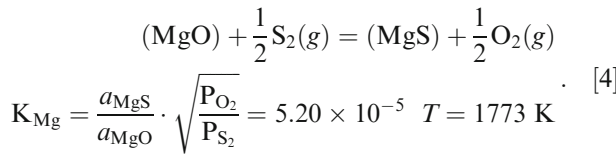
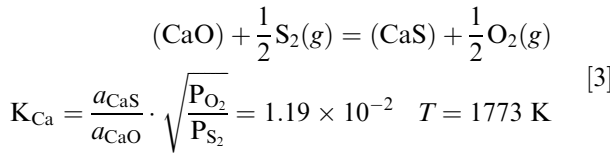


Fig. 6—Variation of sulfur content in slag with titanium suboxide (Ti_2O_3) under slag-gas equilibrium condition calculated by FactSage.

increase in the M/C ratio, the Ti_2O_3 content did not change, indicating that the Ti_2O_3 content is not the determining factor of the sulfide capacity for slag with a fixed amount of TiO_2 .

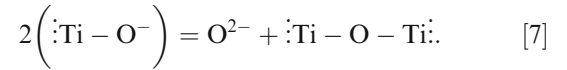
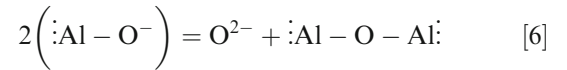
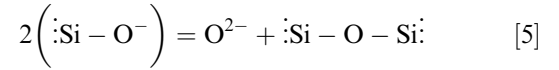
In addition, the equilibrium constant (K) of the slag-gas equilibrium desulfurization reaction of CaO and MgO was calculated by FactSage, and the results are shown in Eqs. [3] and [4]. It is confirmed that MgS is lower stable than CaS under the conditions studied, which are the same as those used in the study by Park *et al.*[26] We also focused on the change in basicity (which represents the change in the free oxygen in slag to some extent), as shown in Figure 8. Analysis of the molar basicity of the CaO-SiO₂-TiO₂-MgO-Al₂O₃ quinary slag system revealed that increasing the TiO_2 content resulted in reduced binary molar basicity, while mass substitution resulted in increasing the quaternary molar basicity ($(\text{CaO} + \text{MgO})/(\text{SiO}_2 + \text{TiO}_2)$). Combined with the change in the binary basicity, we found that when the quaternary molar basicity was less than 0.875, the effect of the quaternary molar basicity dominates, and when the quaternary molar basicity was greater than 0.875, the effectiveness of the binary basicity began to dominate. In other words, titanium dioxide plays an indispensable role in the sulfide capacity transition in the substitution of MgO for CaO.



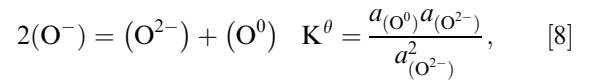
D. Structural Analysis

The sulfide capacity is an indicator closely associated with the slag structure.^[27–29] In basic earth silicate melts containing alumina, when the $\text{Al}_2\text{O}_3/\text{MO}$ (MO = a basicity oxide) ratio is smaller than unity, the coordination structures of aluminum oxide and silicon dioxide are the same, *i.e.*, tetrahedral. Al^{3+} requires charge compensation due to the valence difference relative to that of Si^{4+} , and charge compensation of Ca^{2+} takes higher priority than that of Mg^{2+} .^[30–33] In titania silicate glasses and melts, Ti^{4+} ions can have fourfold coordination in the form of isolated clusters or substituted Si^{4+} , and can also be coordinated to more than four oxygens.^[34] Henderson,^[35] Sandstorm,^[36] and Gregor^[37] reported that in titania silicate glasses, when the concentration of TiO_2 is high, Ti^{4+} dominantly adopts a tetrahedral structure. Consequently, SiO , AlO , and TiO tetrahedrons exist in the $\text{CaO-SiO}_2\text{-TiO}_2\text{-MgO-Al}_2\text{O}_3$ slags. A previous study by Yan^[38] *et al.* proved the applicability of the above structure in slag viscosity modeling. Therefore, we evaluated the applicability of this structure in determining the sulfide capacity.

The reaction in the slag can be reduced to a combination of basic metal ions (Mg^{2+} and Ca^{2+}) and three kinds of tetrahedral ($[\text{SiO}_4]^{4-}$, $[\text{AlO}_4]^{5-}$, and $[\text{TiO}_4]^{4-}$) species. In other words, the following three main polymerization reactions occur in the slag:



This is actually the polymerization of three oxygens reported by Fincham and Richardson^[39]:



where O^- is non-bridging oxygen, O^{2-} is free oxygen, and O^0 is bridging oxygen. Considering Eq. [8], as the equilibrium constant increases, the degree of melt polymerization increases.

From Eq. [1], the desulfurization of slag has an effect on the exchange of free oxygen in the slag and metal sulfur ions or gas sulfur. The basicity of slag and the temperature indirectly affect the free oxygen and sulfide capacity. Therefore, it is quite feasible and convenient to directly explore the change in free oxygen content, and thus, the sulfide capacity from the depolymerization reaction of the three oxygen species.

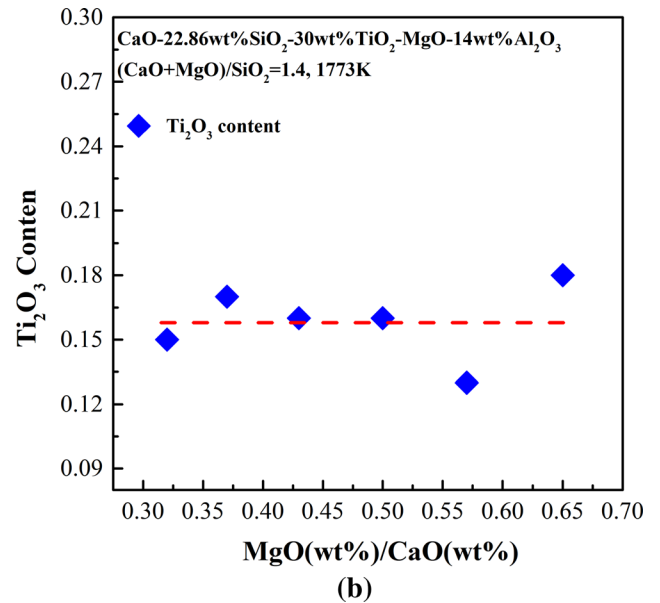
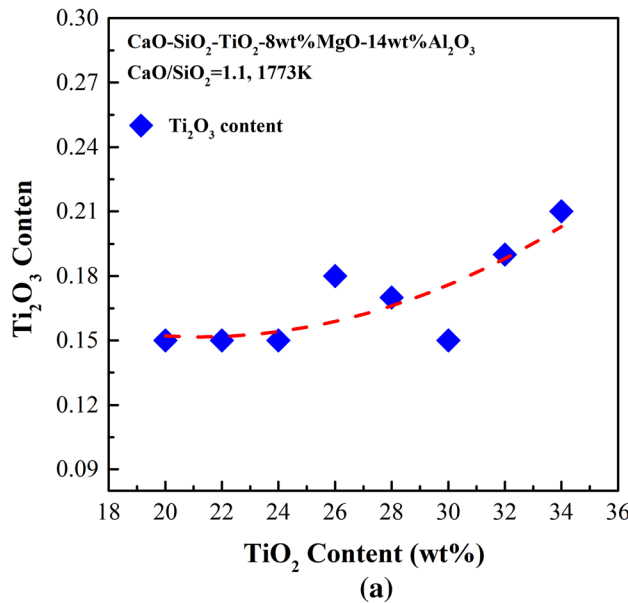


Fig. 7—Variation of Ti_2O_3 content changing with (a) TiO_2 content and (b) M/C ratio.

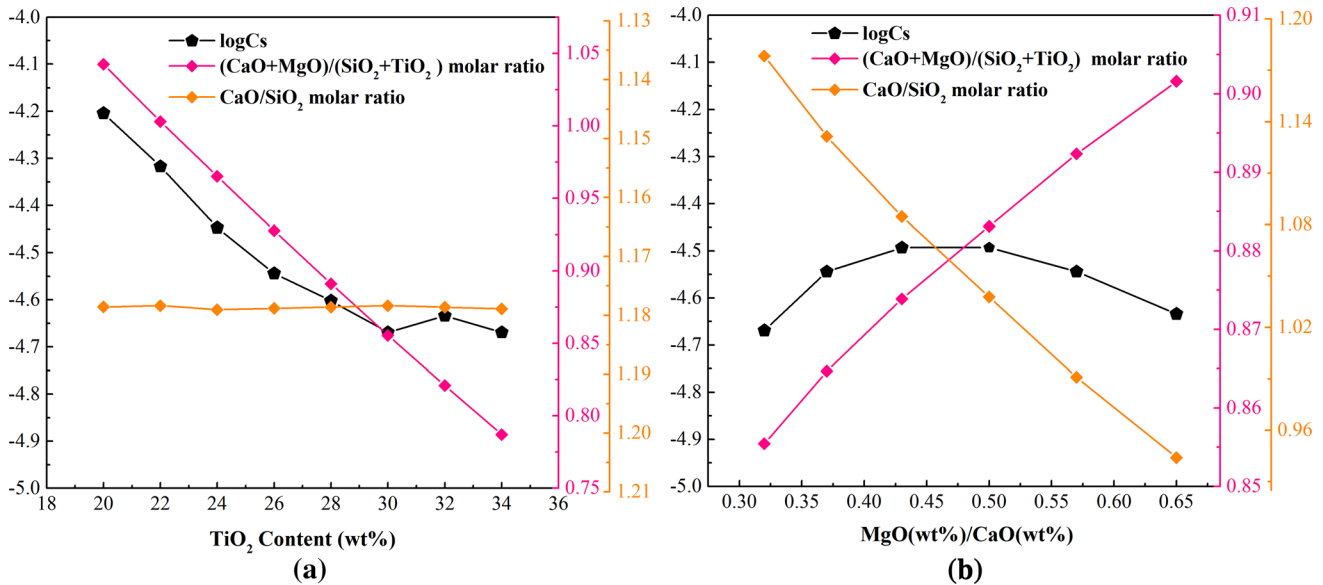


Fig. 8—Quaternary molar basicity and binary molar basicity change with (a) TiO_2 content and (b) M/C ratio.

For the $\text{CaO-SiO}_2\text{-TiO}_2\text{-MgO-Al}_2\text{O}_3$ quinary slag, the depolymerization reactions and standard energy change for the specific depolymerization reactions^[38] are shown in Figure 9. This indicates that the depolymerization of SiO_2 and TiO_2 is more sensitive to M/C , and the content of Al_2O_3 did not change in this study. Consequently, the structural analysis of Ti and Si was used in this study to characterize the slag, as described below.

As the structure of the slag becomes simpler, the degree of the depolymerization reaction in the slag increases, and the free oxygen content in the slag increases.^[26,29,40] From our previous work,^[6] Raman spectroscopy data and the deconvoluted results for the $\text{CaO-SiO}_2\text{-TiO}_2\text{-MgO-Al}_2\text{O}_3$ slag were obtained, and in the present work, the simple structural units of slag were used to characterize free oxygen in the slag. From the perspective of molten silicate slag,^[41–45] structural information related to the slag can be obtained through Raman spectral analysis and other spectral experimental data, and is usually represented by Q^n (where n is the bridge oxygen number). The higher the content of Q^3 and Q^4 in the slag, the higher the degree of slag polymerization. On the other hand, a higher content of Q^0 , Q^1 , and Q^2 species indicates a higher degree of slag depolymerization. Because Raman spectroscopy only detects a fraction of the coupling SiO_4^{4-} (*i.e.*, Q^0) and $\text{Ti}_2\text{O}_6^{2-}$ chains, the use of Q^0 to represent the simple structure was excluded. In fact, Q^0 is insignificant, as explained below. Therefore, we used the sum of Q^1 and Q^2 to represent the simple structural units of silicon. Due to the super-high TiO_2 content, the structure of Ti^{4+} cannot be ignored. Compared with the $\text{Ti}_2\text{O}_6^{2-}$ structural unit, the TiO_4^{4-} structural unit and the O-Ti-O deformation unit are simpler,^[46,47] and are consistent; thus, TiO_4^{4-} and O-Ti-O were used to represent the simple structural units of titanium slag. Figure 10 shows the fraction of simple structural units of (Si + Ti) and

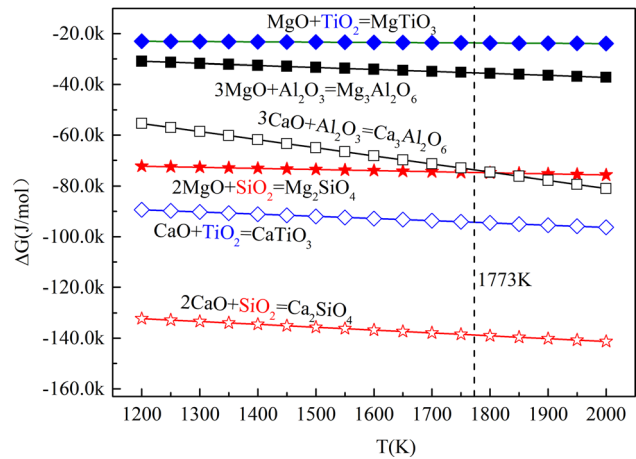


Fig. 9—Standard energy change for the specific depolymerization reactions.

Ti as a function of the (a) TiO_2 content and (b) M/C ratio. The present sulfide capacity and the fraction of simple structural units generally follow the same trend, which is consistent with the previous statement that the amount of free oxygen in the slag can greatly affect the sulfide capacity. In addition, we found that the simple structure of (Ti + Si) varies in a manner that is quite consistent with that of Ti. This could be explained by the deconvoluted Raman data, where among the structural units (Si, Al, Ti) detected by the Raman analysis of the $\text{CaO-SiO}_2\text{-TiO}_2\text{-MgO-Al}_2\text{O}_3$ slag, the silicon structural units accounted for only about 20 pct, which is much less than the content of titanium structural units, which was not less than 50 pct. This proves that the high-titanium slag system cannot be analyzed from the perspective of Si, but must be analyzed from the perspective of Ti, which is the main influence on the high-temperature structure of high TiO_2 slag.

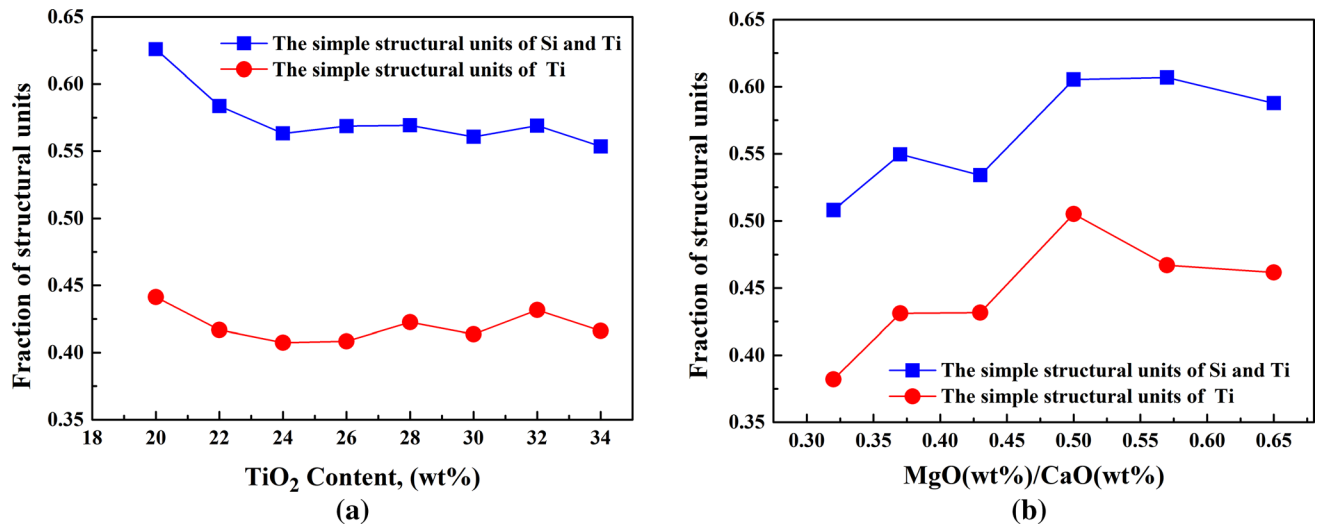


Fig. 10—Fraction of simple structural units of (Si + Ti) and Ti as a function of (a) TiO₂ content and (b) *M/C* ratio.

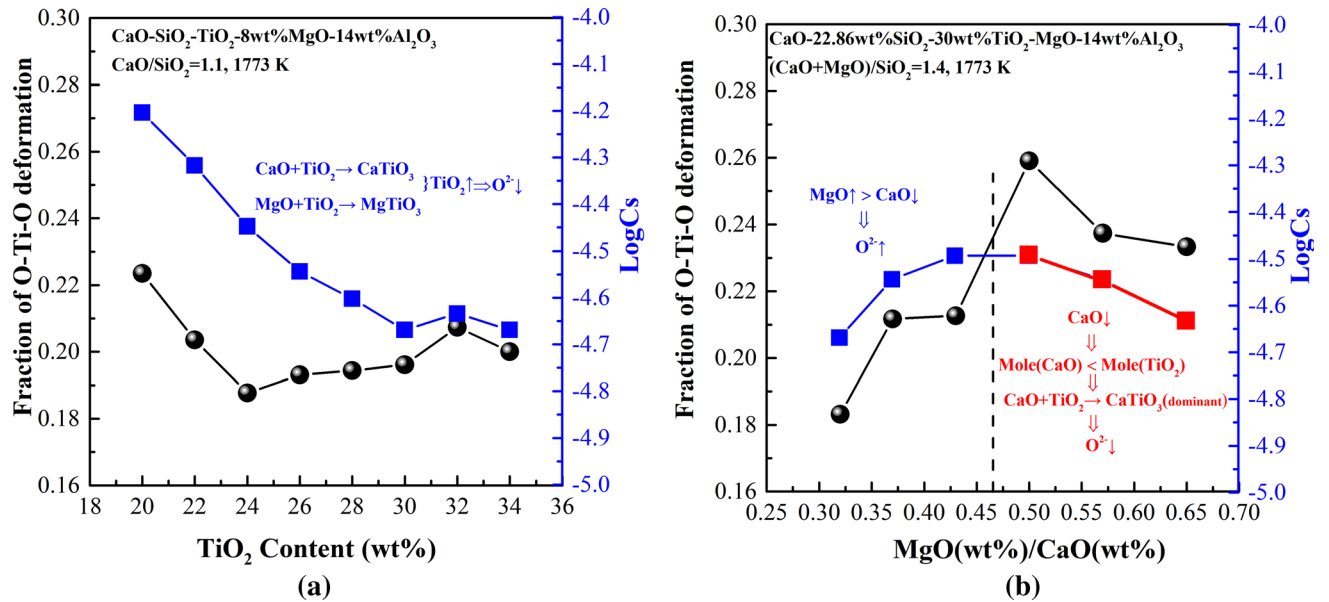


Fig. 11—Sulfide capacity, reaction analysis, and fraction of O-Ti-O deformation units as a function of (a) TiO₂ content and (b) *M/C* ratio.

In titanium-based melts, the depolymerization reaction of Ti has an extremely important effect on desulfurization. The fraction of O-Ti-O deformation units in the slag as a function of the (a) TiO₂ content and (b) *M/C* ratio, and the depolymerization reaction analysis are presented in Figure 11.

The figure indicates that the variation of the fraction of the O-Ti-O deformation units basically follows the same trend as that of logCs. The free oxygen provided by the Ti depolymerization reaction can reflect the overall free oxygen to some extent. With increasing TiO₂ content, the depolymerization of Ti is promoted, which is beneficial to the generation of CaTiO₃ and MgTiO₃ and reduces the content of free oxygen used for

replacing sulfur in the slag. That is, $a_{O^{2-}}$ decreases while f_S^- is basically unchanged, leading to a decrease in the sulfide capacity.

At 1773 K, the Gibbs energy of the depolymerization of Ti with Ca is -94342.6 J/mol, while that of Ti with Mg is -23693.7 J/mol, which means that the depolymerization of Ti with Ca is more sensitive than that of Ti with Mg. When MgO initially substitutes for CaO, the slag contains an excess of CaO, the depolymerization of Ti with Ca is not dominant. Eventually, the increase in the molar amount of MgO due to mass substitution outweighs the reduction of CaO, as shown in Table III, resulting in an increase in the free oxygen in the slag. That is, the increase in $a_{O^{2-}}$ is greater than the increase in

f_{S}^{2-} , thereby increasing the sulfide capacity. With the sequential increase in the M/C ratio, the molar amount of CaO is insufficient for the depolymerization of Ti with Ca, and the depolymerization of Ti with Ca gradually becomes the most influential reaction. Consequently, the free oxygen in the slag declines. In other words, the decrease in a_{O}^{2-} and the increase in f_{S}^{2-} cause the sulfide capacity to decrease.

IV. CONCLUSIONS

The effects of the TiO₂ content and M/C ratio on the sulfide capacity of super-high TiO₂ slag were experimentally studied using the gas-slag phase equilibrium method, and the main conclusions are as follows:

1. In the CaO-SiO₂-TiO₂-MgO-Al₂O₃ slag system, as the content of TiO₂ in the slag increased from 20 to 34 wt pct, the sulfide capacity declined from 6.25×10^{-5} to 2.86×10^{-5} , and when the TiO₂ content exceeded 30 wt pct, the influence on the sulfide capacity became negligible. With an increasing M/C ratio, the slag sulfide capacity followed a non-monotonic trend, where it first increases and then decreased.
2. Thermodynamically, the decrease in the CaO activity reduced of the free oxygen in the slag with increasing TiO₂ content. The increase in titanium suboxide slowed the reduction of the sulfide capacity. Mass substitution mainly influenced the change of free oxygen in the slag, and then the sulfide stability and oxygen concentration worked together, leading to non-monotonic sulfide capacity of the slag in which MgO substitutes for CaO. Focusing on the basicity change, the sulfide capacity was dependent on the effect of both the quaternary molar basicity and binary molar basicity. When the quaternary molar basicity is less than 0.875, the effect of the quaternary molar basicity dominates, and when the quaternary molar basicity is greater than 0.875, the effective binary basicity begins to dominate.
3. Considering structural changes within the CaO-SiO₂-TiO₂-MgO-Al₂O₃ slag system, the anion groups mainly existed in the form of three kinds of tetrahedral ($[\text{SiO}_4]^{4-}$, $[\text{AlO}_4]^{5-}$, and $[\text{TiO}_4]^{4-}$) species. For the high TiO₂ slag, the structure of Ti and the depolymerization reaction of Ti both had an extremely important effect on desulfurization. The change in the fraction of the O-Ti-O deformation units follows basically the same trend as logCs. The present results can be attributed to the depolymerization reaction.

ACKNOWLEDGMENTS

This study was supported by National Key R&D Program of China (Grant No. 2018YFC1900500).

REFERENCES

1. Z. Yuan, X. Wang, C. Xu, W. Li, and M. Kwauk: *Miner. Eng.*, 2006, vol. 19, pp. 975–78.
2. F. Valighazvini, F. Rashchi, and E. Khayyam Nekouei: *Ind. Eng. Chem. Res.*, 2013, vol. 52, pp. 1723–30.
3. Z. Pang, X. Lv, Y. Jiang, J. Ling, and Z. Yan: *Metall. Mater. Trans. B*, 2020, vol. 51B, pp. 722–31.
4. A. Shankar, M. Görnerup, A.K. Lahiri, and S. Seetharaman: *Metall. Mater. Trans. B*, 2007, vol. 38B, pp. 911–15.
5. T. Nagasaka, M. Hino, and S. Ban-Ya: *Metall. Mater. Trans. B*, 2000, vol. 31B, pp. 945–55.
6. Z. Pang, X. Lv, J. Ling, Y. Jiang, Z. Yan, and J. Dang: *Metall. Mater. Trans. B*, 2020, vol. 51B, pp. 2348–57.
7. A. Shankar: *Ironmak. Steelmak.*, 2006, vol. 33, pp. 413–18.
8. A. Shankar, M. Görnerup, S. Seetharaman, and A.K. Lahiri: *Metall. Mater. Trans. B*, 2006, vol. 37B, pp. 941–47.
9. M.K. Cho, J. Cheng, J.H. Park, and D.J. Min: *ISIJ Int.*, 2010, vol. 50, pp. 215–21.
10. G.-H. Park, Y.-B. Kang, and J.H. Park: *ISIJ Int.*, 2011, vol. 51, pp. 1375–82.
11. J.H. Park and G.-H. Park: *ISIJ Int.*, 2012, vol. 52, pp. 764–69.
12. J. Zhang, X. Lv, Z. Yan, Y. Qin, and C. Bai: *Ironmak. Steelmak.*, 2016, vol. 43, pp. 378–84.
13. I. Ghita and H. Bell: *Ironmak. Steelmak.*, 1982, vol. 9, pp. 239–43.
14. S. Brown, R. Roxburgh, I. Ghita, and H. Bell: *Ironmak. Steelmak.*, 1982, vol. 9, pp. 163–67.
15. I.D. Sommerville and H.B. Bell: *Can. Metall. Q.*, 1982, vol. 21, pp. 145–55.
16. M. Ito, K. Morita, and N. Sano: *ISIJ Int.*, 1997, vol. 37, pp. 839–43.
17. C. Che and W. Wang: *Ironmak. Steelmak.*, 1984, vol. 3, p. 004.
18. J. Liu and D. Li: *Eng. Chem. Metall.*, 1987, vol. 1, p. 008.
19. X. Tang and C.S. Xu: *Isij Int.*, 1995, vol. 35, pp. 367–71.
20. H. Bell: *Can. Metall. Q.*, 1981, vol. 20, pp. 169–79.
21. Z. Yan, X. Lv, Z. Pang, W. He, D. Liang, and C. Bai: *Metall. Mater. Trans. B*, 2017, vol. 48B, pp. 2607–14.
22. J.D. Seo and S.H. Kim: *Steel Res.*, 1999, vol. 70, pp. 203–08.
23. K. Karsrud: *Scand. J. Metall.*, 1984, vol. 13, pp. 265–68.
24. K. Karsrud: *Scand. J. Metall.*, 1984, vol. 13, pp. 144–50.
25. R.J. Hawkins, G.S. Meherali, and M.W. Davies: *Ironmak. Steelmak.*, 1971, vol. 209, pp. 646–57.
26. Y.-B. Kang and J.H. Park: *Metall. Mater. Trans. B*, 2011, vol. 42B, pp. 1211–17.
27. L. Wang, Y. Wang, K.-C. Chou, and S. Seetharaman: *Metall. Mater. Trans. B*, 2016, vol. 47B, pp. 2558–63.
28. L.-J. Wang, M. Hayashi, K.-C. Chou, and S. Seetharaman: *Metall. Mater. Trans. B*, 2012, vol. 43B, pp. 1338–43.
29. S. Lee and D.J. Min: *J. Am. Ceram. Soc.*, 2018, vol. 101, pp. 634–43.
30. J.H. Park, D.J. Min, and H.S. Song: *Metall. Mater. Trans. B*, 2004, vol. 35B, pp. 269–75.
31. K.C. Mills: *ISIJ Int.*, 1993, vol. 33, pp. 148–55.
32. Q. Shu: *Steel. Res. Int.*, 2009, vol. 80, pp. 107–13.
33. G. Zhang, K. Chou, and K. Mills: *Metall. Mater. Trans. B*, 2014, vol. 45B, pp. 698–706.
34. B.O. Mysen and P. Richet: *Silicate Glasses and Melts: Properties and Structure*, 1st ed., Elsevier, San Diego, 2005, pp. 322–26.
35. G.S. Henderson, X. Liu, and M.E. Fleet: *Phys. Chem. Miner.*, 2002, vol. 29, pp. 32–42.
36. D.R. Sandstrom, F.W. Lytle, P.S.P. Wei, R.B. Gregor, J. Wong, and P. Schultz: *J. Non-Cryst. Solids*, 1980, vol. 41, pp. 201–07.
37. R.B. Gregor, F.W. Lytle, D.R. Sandstrom, J. Wong, and P. Schultz: *J. Non-Cryst. Solids*, 1983, vol. 55, pp. 27–43.
38. Z. Yan, R.G. Reddy, X. Lv, Z. Pang, and W. He: *Ironmak. Steelmak.*, 2018, pp. 1–7.
39. C.J.B. Fincham and F.D. Richardson: *Proc. R. Soc. Lond. Ser. A*, 1954, vol. 223, pp. 40–62.
40. Z. Ren, X. Hu, and K. Chou: *J. Iron Steel Res. Int.*, 2013, vol. 20, pp. 21–25.
41. B.O. Mysen and P. Richet: *Silicate Glasses and Melts*, Elsevier, Amsterdam, 2005.

42. B.O. Mysen: *Eur. J. Miner.*, 2003, vol. 15, p. 781.
43. B.O. Mysen: *Phys. Earth Planet. Int.*, 1998, vol. 107, p. 23.
44. J.H. Park and J. Non-Cryst: *Solids*, 2012, vol. 358, pp. 3096–3102.
45. J.H. Park: *Met. Mater. Int.*, 2013, vol. 19, pp. 577–84.
46. K. Zheng, Z. Zhang, L. Liu, and X. Wang: *Metall. Mater. Trans. B*, 2014, vol. 45, pp. 1389–97.

47. J. Ryerson: *Am. Miner.*, 1980, vol. 65, pp. 1150–65.

Publisher's Note Springer Nature remains neutral with regard to jurisdictional claims in published maps and institutional affiliations.